

Analysis of a Kepler Light Curve of the Novalike Cataclysmic Variable KIC 8751494

Taichi KATO

Department of Astronomy, Kyoto University, Sakyo-ku, Kyoto 606-8502
tkato@kusastro.kyoto-u.ac.jp

and

Hiroyuki MAEHARA

*Kiso Observatory, Institute of Astronomy, School of Science, The University of Tokyo 10762-30, Mitake, Kiso-machi,
Kiso-gun, Nagano 397-0101*
maehara@kiso.ioa.s.u-tokyo.ac.jp

(Received 201 0; accepted 201 0)

Abstract

We analyzed a Kepler light curve of KIC 8751494, a recently recognized novalike cataclysmic variable in the Kepler field. We detected a stable periodicity of 0.114379(1) d, which we identified as being the binary's orbital period. The stronger photometric period around 0.12245 d, which had been detected from the ground-based observation, was found to be variable, and we identified this period as being the positive superhump period. This superhump period showed short-term (10–20 d) and strong variations in period most unexpectedly when the object entered a slightly faint state. The fractional superhump excess varied as large as $\sim 30\%$. The variation of the period very well traced the variation of the brightness of the system. The time-scales of this variation of the superhump period was too slow to be interpreted as the variation caused by the change in the disk radius due to the thermal disk instability. We interpreted that the period variation was caused by the varying pressure effect on the period of positive superhumps. This finding suggests that the pressure effect, in at least novalike systems, plays a very important (up to $\sim 30\%$ in the precession rate) role in producing the period of the positive superhumps. We also described a possible detection of the negative superhumps with a varying period of 0.1071–0.1081 d in the Q14 run of the Kepler data, and found that the variation of the frequency of the negative superhumps followed that of positive superhumps. The relation between the fractional superhump excesses of negative and positive superhumps can be understood if the angular frequency of the positive superhumps is decreased by a pressure effect. We also found that the phase of the velocity variation of the emission lines reported in the earlier study is compatible with the SW Sex-type classification. Further, we introduced a new two-dimensional period analysis using least absolute shrinkage and selection operator (Lasso) and showed superior advantage of this method.

Key words: accretion, accretion disks — stars: dwarf novae — stars: individual (KIC 8751494) — stars: novae, cataclysmic variables

1. Introduction

Cataclysmic variables (CVs) are close binary systems consisting of a white dwarf and a mass-transferring red dwarf star. The accreted matter forms an accretion disk around the white dwarf unless the magnetic field of the white dwarf is sufficiently strong. CVs with accretion disks are classified into dwarf novae (DNe), which show outbursts with amplitudes of 2–8 mag, and novalikes, which do not show strong outbursts. The distinction between these systems are believed to be a result of the thermal instability in the accretion disk, and novalike variables are regarded as systems having higher mass-transfer rates than in DNe, resulting in thermally stable accretion disks (see e.g. Osaki 1996).

Superhumps are variations whose periods are longer (these superhumps are therefore also called positive superhumps) than the orbital period by a few percent,

and are observed during superoutbursts of SU UMa-type dwarf novae (a class of dwarf novae) and in some novalike variables (Patterson, Richman 1991; Patterson 1999). These superhumps are believed to arise from the precessing non-axisymmetric disk whose eccentricity is produced by the tidal instability arising from the 3:1 resonance (Whitehurst 1988; Hirose, Osaki 1990). The fractional superhump excess ($\epsilon \equiv P_{\text{SH}}/P_{\text{orb}} - 1$ in period and $\epsilon^* \equiv 1 - P_{\text{orb}}/P_{\text{SH}}$ in frequency, where P_{SH} and P_{orb} are the superhump period and the orbital period, respectively) is an observational measure of the precession rate of the accretion disk. If we treat the precessing disk dynamically, and ignore hydrodynamical effects, ϵ^* is shown to have a form (Osaki 1985):

$$\epsilon^* = \frac{\omega_{\text{prec}}}{\omega_{\text{orb}}} = \frac{3}{4} \frac{q}{\sqrt{1+q}} \left(\frac{R_d}{A} \right)^{3/2}, \quad (1)$$

where $q = M_2/M_1$ is the mass ratio of the binary, ω_{prec} and ω_{orb} are the precessional and orbital angular velocity, and R_d and A are the disk radius and the binary separation, respectively. This value was reported to be larger than the observed values (e.g. Molnar, Kobulnicky 1992) and it has been shown that the pressure also affects ω_{prec} [see Lubow (1992); Hirose, Osaki (1993). Murray (1998); Montgomery (2001); Pearson (2006) also discuss implications]. The pressure effect, however, has been usually regarded as of secondary importance for analysis of superhump data in dwarf novae because the order of magnitude estimate suggested that the gravitational effect of the secondary is much larger than the pressure effect (see Osaki 1985). We here report the discovery of rapid period variation of the period of positive superhumps in a nova-like variable in the Kepler (Borucki et al. 2010; Koch et al. 2010) field, whose variation can be better understood as a result of the pressure effect.

This object [KIC 8751494; since the object is located at $19^{\text{h}}24^{\text{m}}10^{\text{s}}.81$, $+44^{\circ}59'34''.9$, it is also referred to as KIC J192410.81+445934.9 (Williams et al. 2010); we hereafter use an abbreviation KIC J1924] is a nova-like CV discovered in the Kepler field (Williams et al. 2010). Using ground-based photometry and spectroscopy, Williams et al. (2010) identified an orbital period of 0.12233(7) d. Based on the narrow hydrogen emission lines and the presence of strong HeII and CIII/NIII emission lines, Williams et al. (2010) suggested that this object may be a member of SW Sex stars [for a recent summary of SW Sex stars, see e.g. Rodríguez-Gil et al. (2007a), Rodríguez-Gil et al. (2007b)].

Since the Kepler data greatly improved our understanding in KIC J1924, we first give the characterization of this system in section 2 and then describe our interpretation of the period variation of the positive superhumps in section 3.

2. Characterization of KIC J1924

2.1. Long-Term Variation

We used Kepler public SC data (parts of Q2 and Q3 quarters and the full Q5 quarter) and LC data (Q2, Q3, Q5–Q10 and Q14) for analysis. The long-term light curve (figure 1) indicates that the object entered a slightly low state 0.5 mag (2011 April–May) below the brightest observations in Kepler. The object showed a gradual decline to this minimum since the later half of 2010 and was slowly rising from this minimum until the end of the observation (2011 September). The fading was very shallow compared to those of VY Scl-type objects (cf. Greiner 1998; Leach et al. 1999). The SC data were obtained around the brightest epochs in the available Kepler data.

This object has a close apparent companion (g -magnitude 16.71 and separation $6''.8$ according to the Kepler Input Catalog). Because the Kepler has a pixel size of $4''$ and is defocused to obtain better a signal-to-noise ratio for brighter objects, this close companion contaminates the observed synthetic aperture counts. We estimated this effect by measuring the variation of the

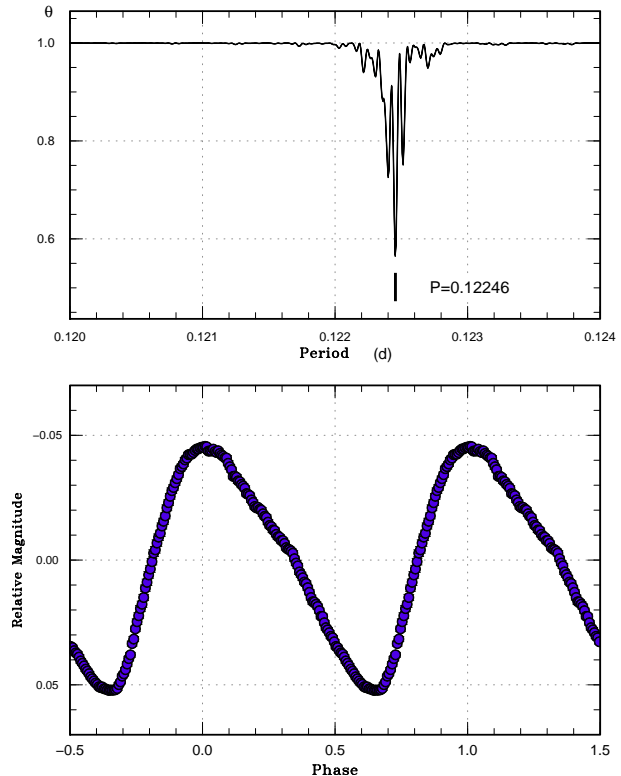


Fig. 2. Mean superhump profile of KIC J1924 from the SC data. (Upper): PDM analysis. (Lower): Phase-averaged profile.

centroid coordinates of KIC J1924 toward the direction of the companion. The measured variation was $0''.4$. This value and the direction of the centroid’s movement can be well explained assuming that the companion contributes $1100 \text{ electrons s}^{-1}$ to the centroid’s variation. This estimate of the contribution of the companion indicates that the real range of variation of KIC J1924 was 0.65 mag assuming that the companion has a constant magnitude.

2.2. Orbital Period and Superhump Period

After removing long-term trends, a phase dispersion minimization (PDM; Stellingwerf 1978) analysis yielded the strongest signal at a period (hereafter P_1) of 0.1224555(1) d (SC data, figure 2) and 0.1224533(1) d (LC data, figure 3). Although this signal is similar to the one recorded by Williams et al. (2010), we did not regard this signal as the orbital period, because there are a variation in period between quarters (table 1) and a large systematic $O - C$ variation against a constant period (figure 4). We regard the strongest signal as the superhump period (P_{SH}), whose possibility was already mentioned in Williams et al. (2010).

There is the second strongest signal the period of which is $\sim 7\%$ shorter than P_1 . We call this period P_2 . This period was detected in individual SC runs. Although the period was present in the individual LC runs, the period was difficult to measure because of interference affected by nearly constant sampling intervals in Kepler. When

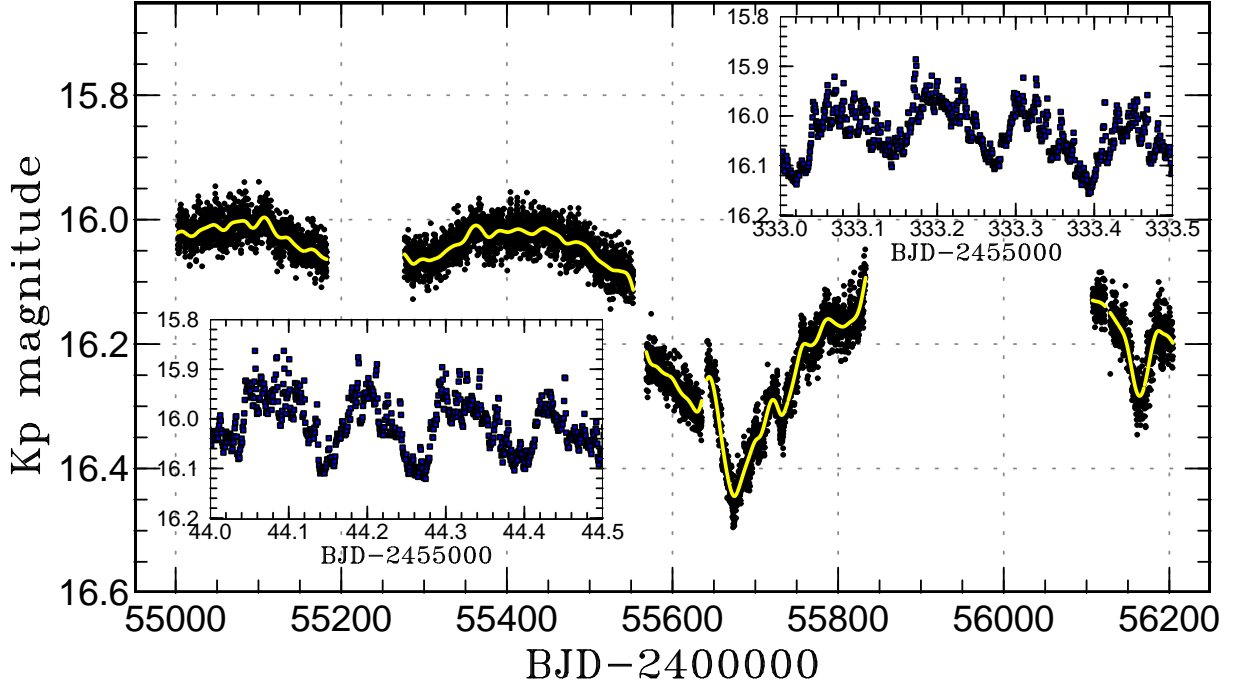


Fig. 1. Long-term light curve of KIC J1924. Both SC and LC data were used. The data were averaged to bins having widths of the orbital period. The Kepler (Kp) magnitudes were estimated while assuming magnitude 12 for 10^7 electrons for an SC (Cannizzo et al. 2010). There are no globally stable zero-points in the Kepler data, and the light curves show discontinuous jumps or drops between different quarters. In the middle of the points the long-term trend is overplotted. Two representative enlarged SC light curves are shown in the insets. The modulations seen in these SC light curves are mainly superhumps.

Table 1. Detected periods in KID J1924 in each quarter.

cadence type	cadence	BJD-2455000		P_1^*	amp [†]	P_2^*	amp [†]
		start	end				
SC	Q2	33.32	63.30	0.1224567(11)	438	0.114279(26)	58
SC	Q3	93.21	123.56	0.1225151(10)	424	0.114319(18)	57
SC	Q5	276.48	371.17	0.1224255(2)	432	0.114376(13)	35
LC	Q2	2.52	91.47	0.1224689(9)	395	— [‡]	56
LC	Q3	93.22	182.50	0.1225044(7)	426	— [‡]	67
LC	Q5	276.49	371.16	0.1224262(7)	432	— [‡]	80
LC	Q6	372.47	462.30	0.1224551(7)	492	— [‡]	71
LC	Q7	463.17	523.23	0.1224923(13)	482	— [‡]	124
LC	Q8	524.15	635.34	0.1225825(2)*	436	— [‡]	52
LC	Q9	641.52	738.93	— [§]	— [§]	— [‡]	38
LC	Q10	739.85	833.27	0.1225383(5)	229	— [‡]	52
LC	Q14	1107.14	1204.32	— [§]	— [§]	— [‡]	64
LC	Q2+Q3	2.52	182.50			0.114376(9)	
LC	Q5+Q6	276.48	462.30			0.114368(12)	
LC	Q7+Q8	463.17	635.34			0.114374(9)	
LC	Q9+Q10	641.52	833.27			0.114379(8)	
SC	all	33.32	371.17	0.1224555(1)		0.1143794(7)	
LC	all	2.52	1204.32	0.1224522(4)		0.114378(3)	

*The values in the parentheses are 1σ errors.

[†]Amplitude in electrons s^{-1} . In determining the amplitudes of P_2 in the LC data, we assumed a period of 0.114379 d.

[‡]Although the signal was present, the period was not well determined due to the interference by the Kepler sampling frequency.

[§]The period or amplitude could not be measured due to the strong variation of the period during this quarter.

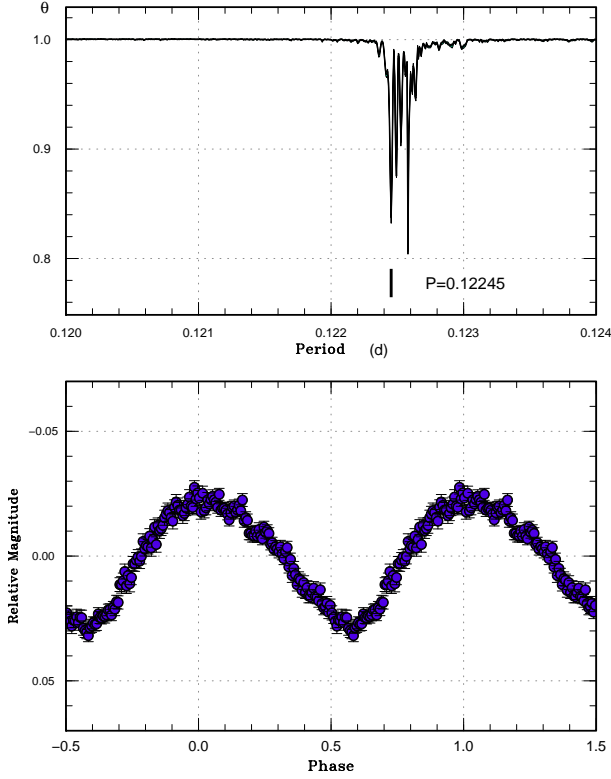


Fig. 3. Mean superhump profile of KIC J1924 from the LC data. (Upper): PDM analysis. The period at 0.12258 d is an artificial signal caused by 1/6 of the intervals of LC data. (Lower): Phase-averaged profile.

two adjacent LC runs were combined, we could also measure P_2 in LC runs (table 1; the periods were determined with the PDM method and the errors are 1σ error by Fernie 1989, Kato et al. 2010). Since P_1 could be measured in most individual LC runs, we did not measure P_1 for the combined adjacent LC runs. For comparison, we also listed P_1 and P_2 measured using all of the data. These measurements indicate that P_2 was constant between different quarters and we regard this period as the orbital period. The period is in good agreement with the ones, derived from two combined LC and SC data (LC data have an advantage of larger cycle numbers, while SC data have higher time resolution, and they are complementary), we adopted a period of 0.114379(1) d by combining these measurements. The mean orbital profile based on the SC data is shown in figure 5. The profile is more symmetric than that of the superhumps. The epoch of the maximum brightness corresponds to BJD 2455228.2463 (the epoch was chosen as the nearest one to the average of the SC observation).

The mean amplitudes of P_1 and P_2 during Q2–Q7 (bright state) were 0.10 mag ($430 \text{ electrons s}^{-1}$) and 0.014 mag ($57 \text{ electrons s}^{-1}$). The mean amplitudes of these signals in individual quarters are given in table 1. The resultant periods yielded a fractional superhump excess ϵ of 7.06% (mean value).

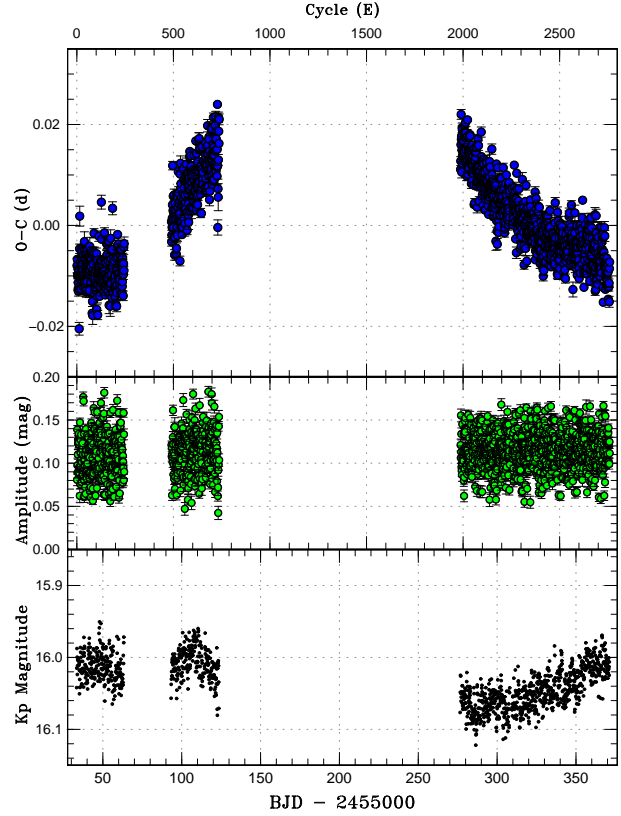


Fig. 4. $O-C$ diagram of superhumps in KIC J1924 in Kepler SC data. (Upper): $O-C$ diagram. The residuals were shown against $\text{Max}(\text{BJD}) = 2455033.500 + 0.122455E$. In extracting the times of superhump maxima, we used a method in Kato et al. (2009) using a mean profile of superhumps in KIC J1924. (Middle): Amplitudes. We used ± 0.4 phase around the maximum for fitting, and the amplitudes shown on the figures are not maximum-to-minimum difference. (Lower): Light curve. Kepler magnitudes were averaged to each superhump cycle.

2.3. Two-Dimensional Period Analysis using Least Absolute Shrinkage and Selection Operator (Lasso)

We here introduce a new method to calculate two-dimensional power spectra using least absolute shrinkage and selection operator (Lasso, Tibshirani 1996), which was introduced to analysis of astronomical time-series data (Kato, Uemura 2012). In Fourier-type period analysis, there is the well-known Heisenberg-Gabor limit, that is, one cannot simultaneously localize a signal in both the time domain and the frequency domain; this characteristic of Fourier-type period analysis is disadvantageous to the analysis of such rapidly changing periods, as superhumps in outbursting dwarf novae have. The advantage of the Lasso analysis is that this method is not restricted by the Heisenberg-Gabor limit and the peaks in the power spectra are very sharp.¹ There is, however, a set-back of this method that the resultant power is not linear in power amplitude. It is very advantageous to use the Lasso period

¹ A simple explanation why the Lasso-type analysis can overcome the Heisenberg-Gabor limit in a different field of science can be found in Herman, Strohmer (2009).

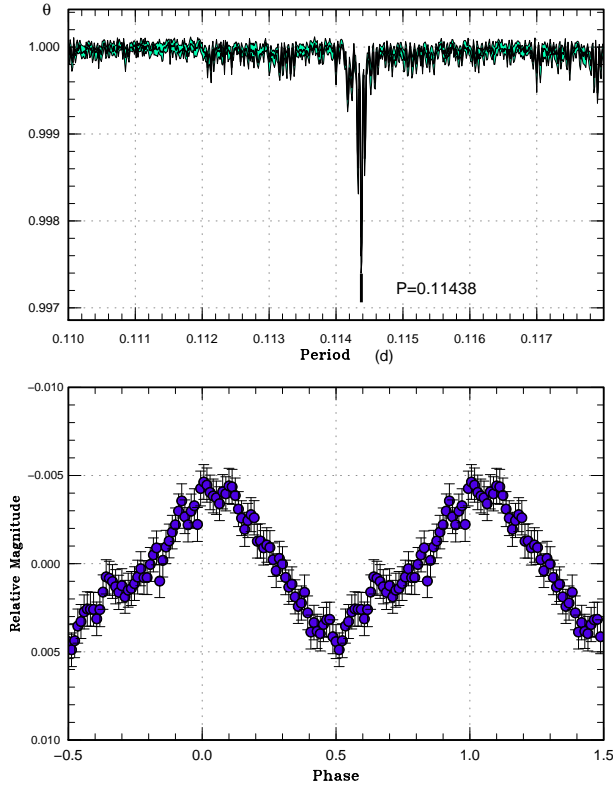


Fig. 5. Orbital variation of KIC J1924 from the SC data. (Upper): PDM analysis. (Lower): Phase-averaged profile.

analysis in resolving closely spaced signals when we know that only a small number of signals coexist. Lasso gives very sharp signals in the two-dimensional power spectra, and thus it is suitable for studying the signals with rapidly varying frequency, such as superhumps in outbursting SU UMa-type dwarf novae (e.g. Osaki, Kato 2013b).

The power spectra were estimated obtained by applying the method of Kato, Uemura (2012) to 10 d bins, which were shifted in a step of 1 d after removing the long-term trend using locally-weighted polynomial regression (LOWESS, Cleveland 1979). The 200 frequencies were evenly spaced between frequencies 7.69 and 9.52 c/d to extract the spectra.

There is a free parameter λ in giving an ℓ_1 term (cf. Kato, Uemura 2012). In producing figures 6, 7, we selected λ which gives the signals best contrasted against a background, i.e. the most physically meaningful parameter. This parameter λ is close to the most regularized model with a cross-validation error within one or two standard deviations of the minimum (cf. R Sct for Kato, Uemura 2012). We also applied smearing of the signals between ± 3 bins shifted in a step of 1 d while considering the width of the window.

The resultant spectrum is shown in figures 6 and 7. The latter figure also shows a comparison between Lasso and Fourier analyses. A similar analysis to the SC data yielded a similar result with a better time-resolution. Since there was no additional remarkable feature in the analysis of the SC data, we omitted this figure.

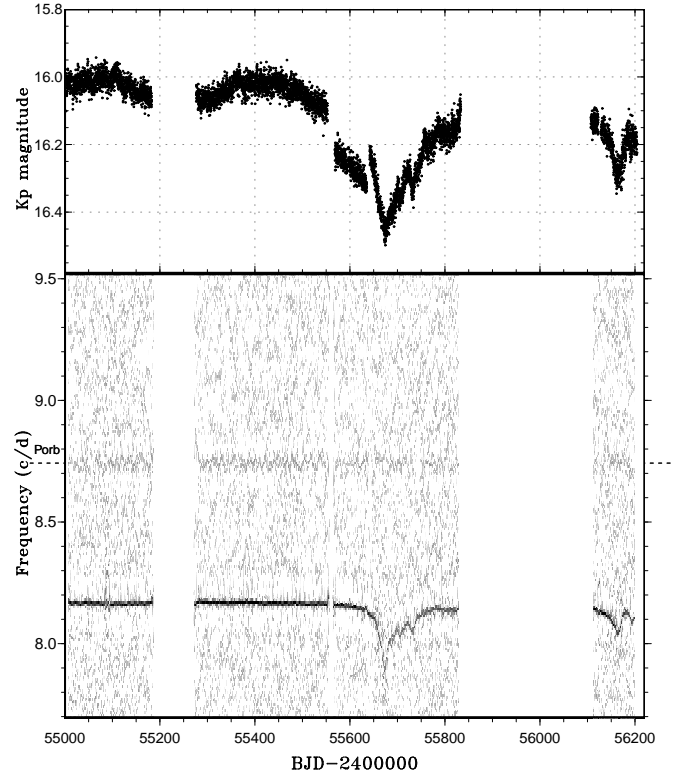


Fig. 6. Lasso 2-D power spectrum analysis of KIC J1924 from the LC data. (Upper): Light curve. The Kepler data were binned to the mean superhump period. (Lower): Result of the lasso analysis ($\log \lambda = -4.8$). The superhump period was discovered to be a signal with a variable frequency, while the orbital period was discovered to be a constant frequency.

2.4. KIC J1924 as an SW Sex Star

Although it is not clear which orbital phase corresponds to the optical maximum of the orbital variation, it can be the phase of the the superior conjunction of the secondary if the maximum represents the reflection effect. We therefore define here the orbital phase of the optical maximum as 0.5 to make a comparison with eclipsing SW Sex stars. The spectroscopic zero phase (red-to-blue crossing of the velocities of the emission lines) $T_{0,\text{spec}} = 24454734.66646(383)$ (Williams et al. 2010) corresponds to an orbital phase of 0.20 (the accumulative error of the phase resulting from the error in the period is smaller than 0.04 even assuming an extreme error of 10^{-5} d). If the emission line traces the motion of the white dwarf, this phase should be close to zero, and this phase delay of the Balmer lines appears to qualify one of the SW Sex-type properties.

The optical spectrum of KIC J1924 is characterized by broad absorption lines apparently arising from the optically thick accretion disk (figure 4 in Williams et al. 2010). Although this kind of “UX UMa-type” spectrum [cf. Warner (1995) for the type definition; Dhillon et al. (2013) suggests that whether the lines are seen in emission or in absorption may be an inclination effect and

proposed to combine UX UMa-type and RW Tri-type with pure emission lines into the UX UMa-type novalike star] is relatively rarely seen in SW Sex stars (see figure 2 in Rodríguez-Gil et al. 2007a), there are some known SW Sex-type object showing the broad Balmer absorption component: HL Aqr (Hunger et al. 1985), LN UMa (Hillwig et al. 1998; Rodríguez-Gil et al. 2007b). A flux calibrated low-resolution spectrum of KIC J1924 is also shown in Østensen et al. (2010), which can be more directly comparable to other SW Sex-type stars.

Improved time-resolved optical spectroscopy, which will provide an independent measure of the orbital period would test the results of the paper, and provide a more solid classification of this system.

2.5. KIC J1924 as a Permanent Superhumper

KIC J1924 persistently showed positive superhumps, during at least Kepler observations up to 2011 September. The object is thus classified as a permanent superhumper. Since the same superhumps were observed in Williams et al. (2010), the positive superhumps seem to have been very stably seen in this object. The object appears to be very similar to V795 Her, another novalike system in the period gap having a similar orbital period (Patterson, Skillman 1994; Papadaki et al. 2006; Šimon et al. 2012). The superhumps of KIC J1924, however, may be more stable than those in V795 Her (Patterson, Skillman 1994; Papadaki et al. 2006).

In table 2, we list permanent superhumpers having orbital periods similar to that of KIC J1924. The recorded $\epsilon=7.1\%$ is the characteristic value of this P_{orb} . Among these objects, only V442 Oph is known to show ~ 3 mag fading² comparable to typical VY Scl-type variables [see light curves in e.g. Greiner (1998), Leach et al. (1999)].

3. Variation of the Superhump Period

3.1. Rapid Period Variation – Radius Variation?

As shown in figure 6, the frequency of the superhump was almost constant before BJD 2455200. After a gap in the Kepler observation, the frequency started to decrease very gradually. The frequency, however, suddenly showed a drop at around BJD 2455620, when the brightness of the system dropped significantly. The frequency of the superhump signal even reached 7.9 c/d (=0.127 d in period), which marked a large ϵ of 11% (ϵ^* amounted to 10%). The obtained frequencies are perfectly in agreement with those obtained using the PDM, as performed in Osaki, Kato (2013a).

Assuming that ϵ^* for positive superhumps depends on $R_{\text{d}}^{3/2}$ (Osaki 1985), this translates to a $\sim 35\%$ increase in disk radius. Adopting a mean ϵ of 7.1%, we can obtain $q=0.30$ using the $\epsilon-q$ relation in Kato et al. (2009) [the relation in Patterson et al. (2005) yields $q=0.27$]. At this q , the tidal truncation radius is close to that of the 3:1 resonance and the disk is not expected to expand beyond

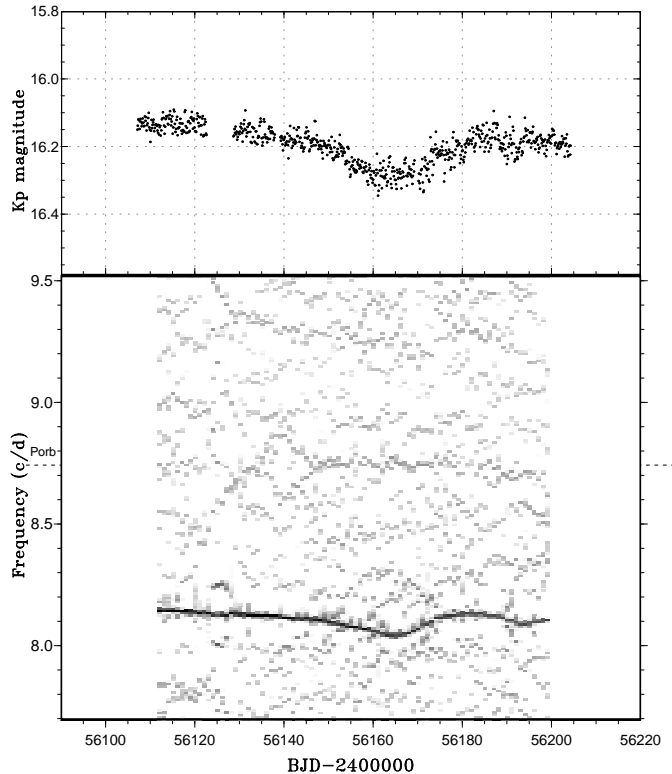


Fig. 8. Period analysis of Q14 data. Short-term variations of the superhump period during another epoch of fading are clearly seen. The signals around frequencies 9.2–9.3 c/d are negative superhumps, whose frequencies also varied in accordance to the system brightness.

the tidal truncation radius for a long time. The radius of the Roche lobe is $\sim 0.50A$. Considering that the radius of the 3:1 resonance is $\sim 0.46A$, it is difficult to ascribe period increase solely to the disk expansion.

3.2. Pressure Effect

We then consider if the dwarf nova-type disk instability can account for the observed variation of the disk radius. The rise time of dwarf nova-type outburst can be expressed as

$$\tau_r = 0.17 \left(\frac{0.1}{\alpha_H} \right) M_1^{1/3} (1+q)^{1/3} P_{\text{orb}}^{2/3} (\text{h}) \text{d} \quad (P_{\text{orb}} \leq 9\text{h}), (2)$$

where τ_r and α_H are the rise time and the viscosity parameter in the hot state, respectively (equation 3.21 in Warner 1995). By using typical values of $M_1=0.8M_{\odot}$, $\alpha_H=0.1$ and assuming $q=0.3$, we obtain $\tau_r \sim 0.3$ d. The decay time is also expressed as

$$\tau_d = 0.75 \left(\frac{0.1}{\alpha_H} \right) M_1^{2/3} (1+q)^{1/6} P_{\text{orb}}^{1/3} (\text{h}) \text{d} \quad (P_{\text{orb}} \leq 9\text{h}), (3)$$

where τ_d is the decay time (equation 3.24 in Warner 1995). The value of τ_d for the same set of parameters is ~ 0.9 d. The both time scales are much shorter than what were seen in subsection 3.1. It is thus unlikely that the period variation is caused by the dwarf nova-type instability.

² See <<http://www.astronurf.com/blazar/variable/UG04/V442%20Oph.html>>.

Table 2. Permanent superhumpers with orbital periods similar to that of KIC J1942.

Object	P_{orb}	P_{SH} (positive)	P_{SH} (negative)	ϵ (%)	SW Sex-type	References
AH Men	0.12721	0.1385	–	8.9	Yes	1,2
V442 Oph	0.12433	–	0.12090	–2.8	Yes	3,4,5
V1084 Her	0.12056	–	0.11696	–3.0	Yes	5,6
V592 Cas	0.115063	0.12228	–	6.3	No	7
KIC J1942	0.114379	0.12245*	0.1071–0.1081	7.1/–5.5 ~ –6.4	Yes	this work
V795 Her	0.108247	0.116486	–	7.6	Yes	8,9,10,11
V348 Pup	0.101839	0.108567	–	6.6	Yes	12,13,14

*Variable period. Mean value.

1: Rodríguez-Gil et al. (2007a), 2: Patterson (1995), 3: Hoard et al. (2000), 4: Hoard, Szkody (2000), 5: Patterson et al. (2002), 6: Rodríguez-Gil et al. (2007b), 7: Taylor et al. (1998), 8: Shafter et al. (1990), 9: Zhang et al. (1991), 10: Casares et al. (1996), 11: Šimon et al. (2012), 12: Rolfe et al. (2000), 13: Rodríguez-Gil et al. (2001), 14: Dai et al. (2010)

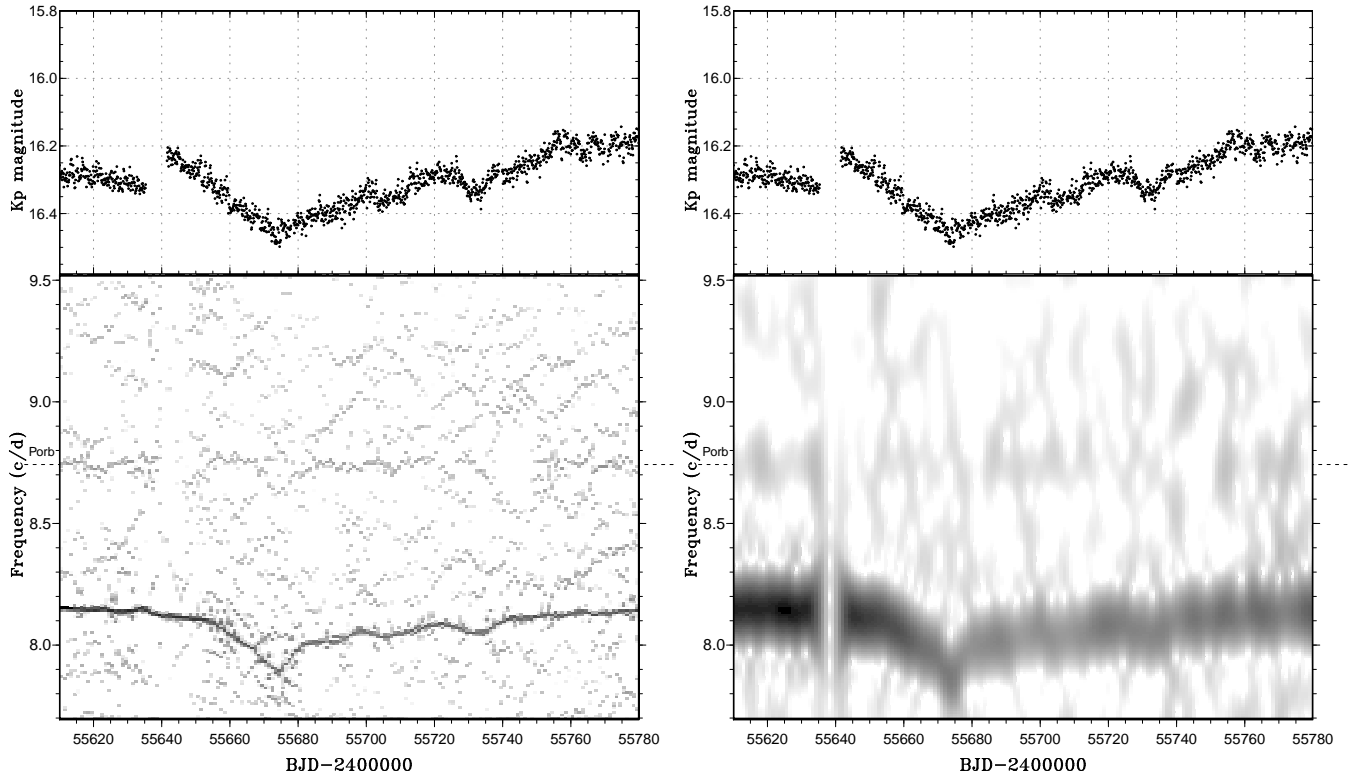


Fig. 7. (Left) Enlargement of figure 6. Short-term variations of the superhump period during the fading are clearly seen. (Right) Discrete Fourier transform of the same data. The advantage of Lasso over Fourier is clearly seen.

In the analysis, up to now we have only used the dynamical term (by the tidal force of the secondary) of producing the precession rate, as approximated in Osaki (1985). It has been shown that the precession frequency is a sum of the dynamical term, the pressure effect (or an effect of a finite thickness of the disk) producing the retrograde precession and a minor wave-wave interaction term (Lubow 1992). Since the variation of the observed superhump period very exactly traced the variation of the system brightness, we suggest that the pressure effect is responsible for the variation of the period. This pressure effect is an increasing function of the sound velocity at the edge of the disk (c_0 ; Hirose, Osaki 1993), which has a dependence of $c_0 \propto \sqrt{T_C}$, where T_C is the temperature of the midplane of the disk. If the disk in a novalike variable can be assumed to be a thermally stable standard disk, the temperature of the midplane has a dependence of $T_C \propto \dot{M}^{3/10}$, where \dot{M} is the mass-transfer rate (equation 5.49 in Frank et al. 2002). The observed luminosity variation of 0.65 mag translates to an $\sim 9\%$ variation of T_C . By using table 1 in Hirose, Osaki (1993) (although this is for a $q = 0.15$ case, we believe that the dependence of q on this estimation is small), a comparison between $c_0 = 0.1$ (realistic novalike disk in a hot state) and $c_0 = 0.085$ yielded an expected ϵ^* variation of $\sim 3\%$. Although this value is smaller than the observed one, this discrepancy might be resolved if the actual disk in a novalike variable in a slightly low state may have a deviation from the steady standard accretion disk. The importance of the pressure effect may be partly attributed to the inferred high mass-transfer rates in SW Sex stars (Rodríguez-Gil et al. 2007a; Townsley, Gänsicke 2009). Since most of the permanent superhumpers are SW Sex stars, this might result a systematic bias if we calibrate the $\epsilon - q$ relation using both dwarf novae and permanent superhumpers.

Following this logic that the period variation of the superhumps can be attributed to the pressure effect, we assumed that the largest ϵ^* was recorded when the disk had the oscillation wave limited to the edge of the accretion disk (corresponding to $c_0 \sim 0$). The precession rate can be expressed as the following equation (Hirose, Osaki 1990):

$$\frac{\omega_{\text{prec}}}{\omega_{\text{orb}}} = \frac{q}{\sqrt{1+q}} \left[\frac{1}{2} \frac{1}{\sqrt{r}} \frac{d}{dr} \left(r^2 \frac{dB_0}{dr} \right) \right], \quad (4)$$

where B_0 is

$$B_0(r) = b_{1/2}^{(0)}/2 = \frac{2}{\pi} \int_0^{\pi/2} \frac{d\phi}{\sqrt{1 - r^2 \sin^2 \phi}}, \quad (5)$$

which is the Laplace coefficient of the order 0 in celestial mechanics (Smart 1953). Numerically calculating this function assuming a radius of the 3:1 resonance of $r_{3:1} = 3^{(-2/3)}(1+q)^{-1/3}$, we could estimate $q = 0.37$ from the largest measured $\epsilon^* = 10\%$. This q is moderately in agreement with the value obtained from the conventional $\epsilon - q$ relation, and we do not consider that our interpretation leads to an obvious contradiction. If the validity of this method is established, observing period variation of positive superhumps in permanent superhumpers will be a tool in estimating mass ratios by using superhumps.

A similar pattern, but with weaker period variations, was also recorded during the Q14 (figure 8).

3.3. Negative Superhumps

During the Q14 run, weak signals of negative superhumps appeared to be present around frequencies of 9.2–9.3 c/d (figure 8). We identified these signals as real ones, because close, non-overlapping bins show similar enhancement of signals. Since these non-overlapping bins share no observations in common, we regarded them as a signature for the independent detection. The signal, however, was weak and it was extremely difficult to obtain a convincing, phase-averaged light curve of this signal due to the variation of the frequency (just like the difficulty in obtaining a period for positive superhumps with period variation), as discussed below, and due to the coarse LC sampling. We describe the properties and implications of the signals assuming that the signals are real. This assumption may be tested by future Kepler observations, especially if SC runs are available. These negative superhumps were not detected in other quarters. The frequency of negative superhump varied as in the same manner as that of positive superhumps; the frequency became smaller when the system slightly faded at around BJD 2455160–2455170 (frequency 9.25 c/d, period 0.1081 d, $\epsilon^* = -5.8\%$) compared to the brighter state around BJD 2456125–2456140 (frequency 9.34 c/d, period 0.1071 d, $\epsilon^* = -6.8\%$). The variation followed a very similar pattern to that of positive superhumps. Since the pressure effect is not expected to work for producing negative superhumps (Osaki, Kato 2013a; see also more detailed discussion in Osaki, Kato 2013b), we can attribute this frequency variation to the change in the radius of the disk. Since ϵ^* has a dependence of $R_d^{3/2}$ (Larwood 1998), this variation of ϵ^* corresponds to a variation of 11% in the radius of the accretion disk. The observation of a lower ϵ^* in a fainter state is consistent with the picture that a disk is expected to be smaller when the mass-transfer rate decreases.

There is a known relationship between ϵ_+^* (positive superhumps) and ϵ_-^* (negative superhumps); that is $\epsilon_+^* \simeq 7/4|\epsilon_-^*|$ [from Larwood (1998); see Osaki, Kato 2013b for detailed discussion; this factor has been observationally known to be close to 2, cf. Patterson et al. (1997); Wood et al. (2009)] and clearly the variation in this object does not follow this relation. This result can also be understood if the ϵ_+^* is suppressed by the pressure effect when the system is bright.

3.4. Variation in Mass-Transfer

It appears that the mass-transfer rate from the secondary in KIC J1924 varied significantly on a time-scale of 10–20 d. These values are much shorter than in typical VY Scl-type stars (the typical low states lasts for months to years). Garnavich, Szkody (1988), however, showed much shorter historical fadings in V442 Oph. This and present finding suggest that mass-transfer rates in novalike systems significantly vary on a time-scale as short as 10–20 d. V795 Her, an object very similar to KIC J1942, did not experience deep low states such as are seen in typical

VY ScI-type stars [Wenzel et al. (1988); this has also been confirmed by recent VSNET (Kato et al. 2004), AAVSO and CRTS (Drake et al. 2009) observations]. V795 Her also showed low-amplitude (up to 1 mag) long-term variations such as were seen in Šimon et al. (2012). It would be interesting to see whether the superhump periods in V795 Her varies in the same way as in KIC J1924.

4. Conclusion

We studied a public Kepler light curve of the nova-like variable KIC 8751494 (KIC J192410.81+445934.9). Although the photometric period (0.12245 d, Kepler data) identified by the ground-based observation has also been confirmed in the Kepler data, we identified it as the superhump period based on the long-term instability of the period. We alternatively identified a weaker, but a stable periodicity of 0.114379(1) d as being the orbital period. The inferred fractional superhump excess of 7.06% (mean value) is typical of the permanent superhump with an orbital period similar to that of this object. Based on the refined orbital ephemeris, we identified a phase shift in the emission lines in a radial velocity study reported earlier, which strengthens the identification of this object as one of SW Sex stars. The period of superhumps showed a very large (up to $\sim 30\%$ in fractional superhump excess) variation when the object faded in 2011 April–May. The variation of the period almost exactly traced the variation of the system brightness. We examined the origin of the variation of the superhump period assuming the disk-radius variation and dwarf nova-type disk instability. Each possibility is difficult to explain the observed variation. We alternatively suggest that the pressure effect in producing the precession rate of the non-axisymmetric disk plays a more important role. This finding suggests that the pressure effect can have an effect up to $\sim 30\%$ in the precession rate, in at least novalike systems. We also describe a possible detection of negative superhumps with a varying period of 0.1071–0.1081 d in the Q14 run, and found that the variation of the frequency of negative superhumps followed that of positive superhumps. The relation between the fractional superhump excesses between negative and positive superhumps can be understood if the angular frequency of positive superhumps is decreased by the pressure effect.

We are grateful to Prof. Yoji Osaki for discussions. This work was supported by the Grant-in-Aid for the Global COE Program “The Next Generation of Physics, Spun from Universality and Emergence” from the Ministry of Education, Culture, Sports, Science and Technology (MEXT) of Japan. We thank the Kepler Mission team and the data calibration engineers for making Kepler data available to the public.

References

- Borucki, W. J., et al. 2010, *Science*, 327, 977
 Cannizzo, J. K., Still, M. D., Howell, S. B., Wood, M. A., & Smale, A. P. 2010, *ApJ*, 725, 1393

- Casares, J., Martínez-Pais, I. G., Marsh, T. R., Charles, P. A., & Lazaro, C. 1996, *MNRAS*, 278, 219
 Cleveland, W. S. 1979, *J. Amer. Statist. Assoc.*, 74, 829
 Dai, Z.-B., Qian, S.-B., Fernández Lajús, E., & Baume, G. L. 2010, *MNRAS*, 409, 1195
 Dhillon, V. S., Smith, D. A., & Marsh, T. R. 2013, *MNRAS*, 428, 3559
 Drake, A. J., et al. 2009, *ApJ*, 696, 870
 Fernie, J. D. 1989, *PASP*, 101, 225
 Frank, J., King, A., & Raine, D. J. 2002, *Accretion Power in Astrophysics: Third Edition* (Cambridge: Cambridge University Press)
 Garnavich, P., & Szkody, P. 1988, *PASP*, 100, 1522
 Greiner, J. 1998, *A&A*, 336, 626
 Herman, M. A., & Strohmer, T. 2009, *IEEE Transactions on Signal Processing*, 57, 2275
 Hillwig, T. C., Robertson, J. W., & Honeycutt, R. K. 1998, *AJ*, 115, 2044
 Hirose, M., & Osaki, Y. 1990, *PASJ*, 42, 135
 Hirose, M., & Osaki, Y. 1993, *PASJ*, 45, 595
 Hoard, D. W., & Szkody, P. 2000, *New Astron. Rev.*, 44, 79P
 Hoard, D. W., Thorstensen, J. R., & Szkody, P. 2000, *ApJ*, 537, 936
 Hunger, K., Heber, U., & Koester, D. 1985, *A&A*, 149, L4
 Kato, T., et al. 2009, *PASJ*, 61, S395
 Kato, T., et al. 2010, *PASJ*, 62, 1525
 Kato, T., & Uemura, M. 2012, *PASJ*, 64, 122
 Kato, T., Uemura, M., Ishioka, R., Nogami, D., Kunjaya, C., Baba, H., & Yamaoka, H. 2004, *PASJ*, 56, S1
 Koch, D. G., et al. 2010, *ApJL*, 713, L79
 Larwood, J. 1998, *MNRAS*, 299, L32
 Leach, R., Hessman, F. V., King, A. R., Stehle, R., & Mattei, J. 1999, *MNRAS*, 305, 225
 Lubow, S. H. 1992, *ApJ*, 401, 317
 Molnar, L. A., & Koblunicky, H. A. 1992, *ApJ*, 392, 678
 Montgomery, M. M. 2001, *MNRAS*, 325, 761
 Murray, J. R. 1998, *MNRAS*, 297, 323
 Osaki, Y. 1985, *A&A*, 144, 369
 Osaki, Y. 1996, *PASP*, 108, 39
 Osaki, Y., & Kato, T. 2013a, *PASJ*, 65, 50
 Osaki, Y., & Kato, T. 2013b, *PASJ*, in press (arXiv astro-ph/1305.5877)
 Østensen, R. H., et al. 2010, *MNRAS*, 409, 1470
 Papadaki, C., Boffin, H. M. J., Sterken, C., Stanishev, V., Cuypers, J., Boumis, P., Akras, S., & Alikakos, J. 2006, *A&A*, 456, 599
 Patterson, J. 1995, *PASP*, 107, 657
 Patterson, J. 1999, in *Disk Instabilities in Close Binary Systems*, ed. S. Mineshige, & J. C. Wheeler (Tokyo: Universal Academy Press), p. 61
 Patterson, J., et al. 2002, *PASP*, 114, 1364
 Patterson, J., et al. 2005, *PASP*, 117, 1204
 Patterson, J., Kemp, J., Saad, J., Skillman, D. R., Harvey, D., Fried, R., Thorstensen, J. R., & Ashley, R. 1997, *PASP*, 109, 468
 Patterson, J., & Richman, H. 1991, *PASP*, 103, 735
 Patterson, J., & Skillman, D. R. 1994, *PASP*, 106, 1141
 Pearson, K. J. 2006, *MNRAS*, 371, 235
 Rodríguez-Gil, P., et al. 2007a, *MNRAS*, 377, 1747
 Rodríguez-Gil, P., Martínez-Pais, I. G., Casares, J., Villada, M., & van Zyl, L. 2001, *MNRAS*, 328, 903
 Rodríguez-Gil, P., Schmidtobreick, L., & Gänsicke, B. T. 2007b, *MNRAS*, 374, 1359

- Rolfe, D. J., Haswell, C. A., & Patterson, J. 2000, *MNRAS*, 317, 759
- Shafter, A. W., Robinson, E. L., Crampton, D., Warner, B., & Prestage, R. M. 1990, *ApJ*, 354, 708
- Smart, W. M. 1953, *Celestial Mechanics* (Longmans: London, New York)
- Stellingwerf, R. F. 1978, *ApJ*, 224, 953
- Taylor, C. J., et al. 1998, *PASP*, 110, 1148
- Tibshirani, R. 1996, *J. R. Statist. Soc. B*, 58, 267
- Townsley, D. M., & Gänsicke, B. T. 2009, *ApJ*, 693, 1007
- Šimon, V., Poláček, C., Štrobl, J., Hudec, R., & Blažek, M. 2012, *A&A*, 540, A15
- Warner, B. 1995, *Cataclysmic Variable Stars* (Cambridge: Cambridge University Press)
- Wenzel, W., Banny, M. I., & Andronov, I. L. 1988, *Mitteil. Veränderl. Sterne*, 11, 141
- Whitehurst, R. 1988, *MNRAS*, 232, 35
- Williams, K. A., et al. 2010, *AJ*, 139, 2587
- Wood, M. A., Thomas, D. M., & Simpson, J. C. 2009, *MNRAS*, pp 2110–2121
- Zhang, E., Robinson, E. L., Ramseyer, T. F., Shetrone, M. D., & Stiening, R. F. 1991, *ApJ*, 381, 534